Evaluation of the Damper Condition in Synchronous Motors through the Analysis of the Transient Stray Fluxes and Currents considering the Effect of the Remanent Magnetism

H. Castro-Coronado, J. Antonino-Daviu, A. Quijano-Lopez, P. Llovera-Segovia, V. Fuster-Roig, L. Serrano-Iribarnegaray and L. Dunai

***Abstract* -- This paper proposes the qualitative and quantitative analysis of stray-flux and current data under starting to detect damper faults in cylindrical rotor synchronous machines. These machines are typically employed in high power applications and their possible outages may imply huge costs for the industries or plants where they operate. The damper cage is a critical part of these machines and a potential source of catastrophic failures. However, few research works have provided feasible alternatives to monitor the condition of such element. This work analyses the viability of analyzing the electromotive force signals induced by the stray-flux in external coil sensors as well as current signals under starting to diagnose damper faults. The results obtained with laboratory machines with different levels of damper damage show that the analyses of those signals can provide very useful information for determining how the damper degrades over time. Moreover, the paper studies the effect of the remanent magnetism over the viability of the approaches and provides solutions to overcome this problem. The conclusions are valuable for field engineers since, nowadays, there are few available solutions that allow monitoring the condition of such element without motor disassembly.**

***Index Terms*—synchronous machines; fault diagnosis; rotor; damper cage; maintenance; reliability; transient analysis; stray-flux.**

I. INTRODUCTION

THE damper cage (or *amortisseur* winding) plays a crucial role in the operation of many wound rotor synchronous machines [1]. It enables the startup of the machine in an asynchronous way, due to the currents that are induced in the damper bars when the stator winding is connected to the grid. In real applications, when the machine reaches a speed near the synchronous speed n_s (typically, within 95% of n_s), the field winding is supplied with a dc current and the machine is auto synchronized. Therefore, the damper is crucial for the starting of such machines. Moreover, the damper cage has other important functions, such as damping the mechanical oscillations due to load variations, limiting the magnetic field harmonics or contributing to enhance the behavior of the machine under short-circuit conditions [1]-[2].

Cylindrical rotor synchronous machines (CRSM) usually have solid rotors. This is often enough to assume the functions of the damper [3]. However, most of these machines incorporate copper or bronze plates with reduced cross-sectional areas that are allocated in the upper part of the slots and that help to the circulation of currents under starting. Occasional breakages in these damper elements may have important repercussions. Apart from making more difficult the motor starting, some detached fragments may stroke parts of the stator winding insulation, leading to damages and occasional shorted turns with subsequent catastrophic effects.

Therefore, it is of paramount importance to monitor the condition of the damper cage, even in CRSM. In spite of the importance of maintaining this element in proper conditions, the available methods in the field are still very rudimentary, if not intrusive. Offline inspections of the rotor with boreoscope cameras are often employed in the industry [4]; these methods do not guarantee the correct determination of the damper condition. On the other hand, some large machines make use of internal air gap flux sensors, which could help in detecting the fault, but that imply the installation of such elements which is not an economic and practical question [5]. Over recent years, some promising methods based on the analysis of the starting current have been proposed both for salient pole [4] and cylindrical rotor synchronous motors [6]. The results of these works have opened a new research line that is focused on the study of different quantities of the machine under the starting. In this regard, the airgap flux behavior under starting had been investigated to detect damper faults [5], [7] and even some very recent papers have studied the effect of damper bar faults over the leakage flux [8].

The present work compares the analyses of motor currents and stray flux signals under starting to detect damper faults in CRSM. The analysis of stray flux data is living a renewed dynamism recently, revealing itself as a very powerful tool for the diagnostic of different faults that are not always reliably detected with other quantities. More specifically, the analysis of stray flux signals under starting has yielded satisfactory results for diagnosing rotor failures in cage [9]

This work was supported by the Spanish 'Ministerio de Ciencia Innovación y Universidades' and FEDER program in the framework of the 'Proyectos de I+D de Generación de Conocimiento del Programa Estatal de Generación de Conocimiento y Fortalecimiento Científico y Tecnológico del Sistema de I+D+i, Subprograma Estatal de Generación de Conocimiento' (ref: PGC2018-095747-B-I00).

H. Castro-Coronado and L. Serrano-Iribarnegaray are with the Departamento de Ingeniería Eléctrica, Universitat Politècnica de València, Camino de Vera s/n, 46022, Valencia, SPAIN (e-mail:lserrano@die.upv.es).

J. Antonino-Daviu, A. Quijano-Lopez, P. Llovera-Segovia and V. Fuster-Roig are with the Instituto Tecnologico de la Energia, Universitat Politècnica de València, Camino de Vera s/n, 46022, Valencia, SPAIN (e-mails: joanda@die.upv.es, aquijano@ite.upv.es, pllovera@ite.upv.es).

L. Dunai is with the Centro de Investigación en Tecnologías Gráficas, Universitat Politècnica de València, Camino de Vera s/n, 46022, Valencia, SPAIN (e-mail: ladu@upv.es).

and wound rotor induction motors [10]. Hence, it is expected that this technique can be also useful to determine the condition of the damper in CRSM. The results included in this work, obtained with laboratory CRSM, help to ratify this conclusion, proving the respective advantages of each quantity for the diagnosis of damper bar failures in such machines. On the other hand, the effect of the remanent magnetism that exists in the rotor of some CRSM is studied: as shown in the paper, this phenomenon may facilitate the self-synchronization of the CRSM even if the field winding is not supplied, making the duration of the starting shorter and, hence, complicating the starting analysis. A solution to allow the application of the proposed methodology even under those circumstances is provided in the paper.

II. Stray-fluxes and Currents Analyses Under Starting

A. Harmonics in the starting current

Previous works proved that the analysis of the current demanded under starting is a useful method to detect damper failures in both salient pole synchronous motors [4] and CRSM [6], [9]. The idea beyond this approach relies on tracking the characteristic time-frequency evolutions followed by certain fault-related components during that transient. More specifically, the identification of the evolution of the lower sideband harmonic (LSH) given by $f\cdot(1-2\cdot s)$ (f=supply frequency and s=slip) as well as the assessment of the amplitude of that harmonic under starting have been proposed as reliable methods to evaluate the condition of the damper [4]. The identification of other harmonics induced in the current signal can also be useful to diagnose damper faults, such as the upper sideband harmonic ($f\cdot(1+2\cdot s)$) or the fault harmonics near the fifth winding harmonic ($f\cdot(5-4\cdot s)$ and $f\cdot(5-6\cdot s)$). All these harmonics follow characteristic trajectories as the slip s varies under an asynchronous-mode startup. The identification of these trajectories in the time-frequency maps resulting from the starting current analysis is a reliable evidence of the presence of the failure. In salient pole synchronous motors, the saliency effect creates similar components, so periodic trending of the fault harmonics' amplitudes is necessary to detect how the damper degrades over time [4].

B. Harmonics in the stray flux under starting

Damper failures have been reported to amplify certain components in the air gap magnetic field [5], [7], which can be also used for the reliable detection of this fault. However, the measurement of air gap flux data implies the installation of internal probes. With regards to the stray flux, recent works related to cage and wound rotor induction motors have shown that certain components are amplified due to rotor asymmetries and, moreover, these components follow particular evolutions during a direct on-line startup [9]-[10]. The components present in the stray flux have different nature (axial/radial) depending on their origin, as justified in [12]-[13]. More specifically, two main groups of components are amplified when rotor faults are present:

- *Axial components*: located at $s\cdot f$ and $3\cdot s\cdot f$. These may also be influenced by other effects such as eccentricities or load-related problems.
- *Radial components*: the most relevant are the sidebands at $f\cdot(1\pm2\cdot s)$. Other higher frequency harmonics such as those induced in the currents are also amplified.

Apart from the previous components, there are also harmonics associated to the rotational frequency f_r that are usually employed to diagnose eccentricities (these harmonics may be also amplified by misalignments but in a lesser extent [14]). These components are located at $f\pm f_r$ or, equivalently, $f\cdot(1\pm(1-s)/p)$ (we will denote them by f_{ecc} (+) and f_{ecc} (-)). Recent works have shown that these components are also amplified due to rotor damages [15].

As it happened with the fault harmonics in the starting current, the previous stray flux components follow characteristic evolutions as the slip changes under a direct on line startup yielding particular time-frequency patterns that can be used for the diagnosis of the fault.

The same reasoning can be also extended to damper fault detection in CRSM. Note that, depending on the position of the sensor that is used to collect flux data, a higher portion of radial or axial flux will be captured and, therefore, the corresponding components (axial or radial) will be better observed in the subsequent time-frequency analyses.

Fig. 1 shows the expected time-frequency evolutions of all the aforementioned components (flux and/or current) under a simulated direct on-line starting of a 4 pole, 1,1 kW motor. The detection of these evolutions with suitable time-frequency tools is the basis of the techniques proposed in this paper to detect damper failures in CRSM.

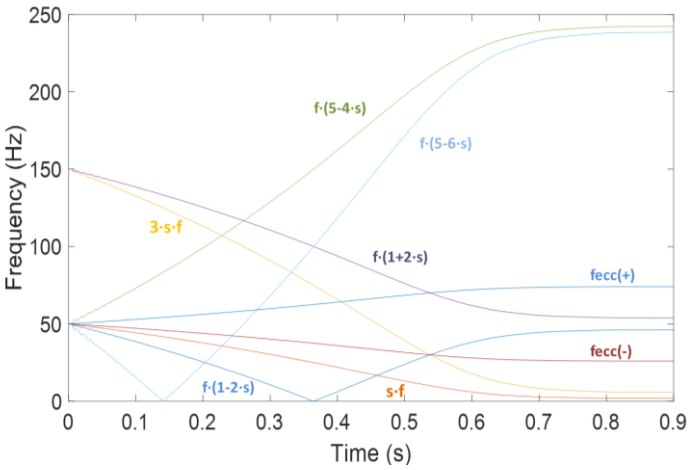

Fig. 1. Expected time-frequency evolutions of the fault components in the flux and/or current signals under starting.

III. Experiments

Several experiments were developed at the laboratory in two different CRSM (CRSM1 and CRSM2) with the following rated characteristics: power =4 kW; number of poles=4; stator voltage=400V; stator current=7.5A; maximum excitation voltage=50V. The specific constructive characteristics of the CRSM windings are detailed next:

- *Stator winding*: double layer winding placed in 48 slots uniformly distributed with a chorded coil span of 9/10 or the pole pitch.
- *Rotor winding*: winding placed in 24 slots with six slots per pole, uniformly distributed in 5/9 of the pole pitch.

- *Damper winding*: constructed as squirrel cage with 36 bars uniformly distributed (9 bars per pole).

Note that the distribution of the damper is uniform in the rotor perimeter while the rotor (field) winding is distributed through 5/9 of the pole pitch, as depicted in Fig.2. This distribution may yield a certain magnetic saliency in the CRSM that will not be so important as in salient-pole synchronous motors [4] but that may yield inherent slight signatures under healthy conditions.

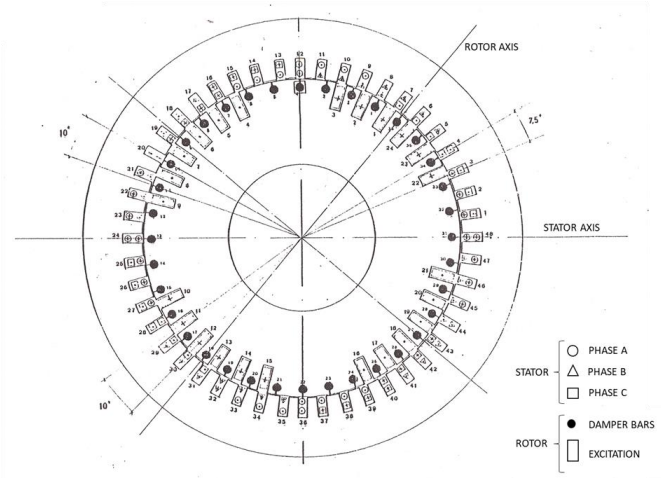

Fig. 2. Emplacement of the different machine windings.

The damper cages of both machines had been subjected to an intense experimentation during more than 40 years of operation. In particular, one of them (CRSM1) was seriously damaged in the past (at least six damper bars were broken and afterwards re-welded). Fig. 3 shows a picture of the rotor and evidence of previous damage in the damper of CRSM1. In the case of CRSM2, despite the intense previous experimentation, which can yield a subsequent wear of the cage, there is no evidence of damper damage.

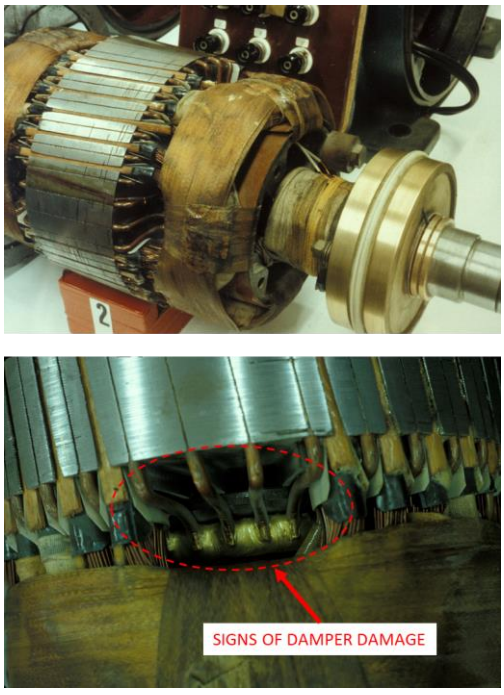

Fig. 3. Rotor of the CRSM and evidence of damper damage in CRSM1.

Different direct-on-line startups were developed for the machine operating under various load conditions, although in the figures only the no load case is shown, since it yields the shortest duration of the starting transient, which is the most critical situation for detecting the evolutions of fault components. In each test, the machine was started in an asynchronous mode (thanks to the damper cage) and, when the steady-state was reached and the speed stabilized, the field winding was supplied (by closing a circuit breaker (C.B.)), hence enabling the synchronization of the motor. The stator current signal was registered (sampling rate f_s=5 kHz). Also, a coil sensor was employed to register the electromotive force (emf) induced by the stray flux under starting. This was an air core coil with N=1000 turns, round shaped and had an external diameter of 80mm and an internal diameter of 39mm It was attached to different positions of the machine frame, so the axial and radial parts of the flux were captured. Fig. 4 shows the laboratory test bench for one of the tested CRSM, as well as its electric scheme. Fig. 5 shows the three coil sensor positions that were tested.

Unlike in CRSM1, the rotor of CRSM2 had a certain level of remanent magnetism which yielded the self-synchronization of the machine, even if the field winding was not supplied (the level of remanent magnetism in each machine was verified by measuring the voltage at the stator terminals while rotating each CRSM without supplying its excitation). In CRSM2, the motor starting was shorter (<1 second) due to the effect of this remanent magnetic field in the rotor.

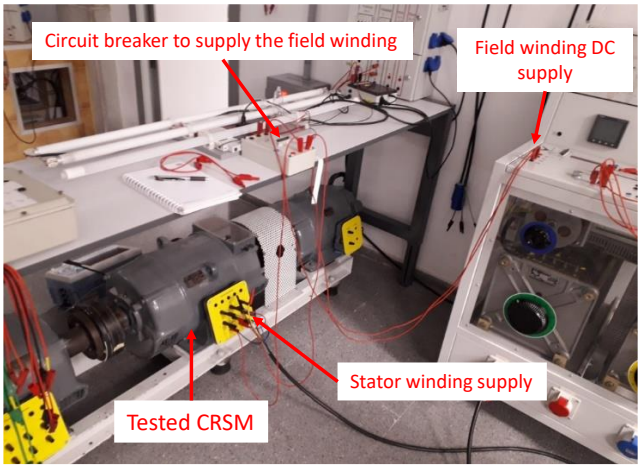

(a)

(b)

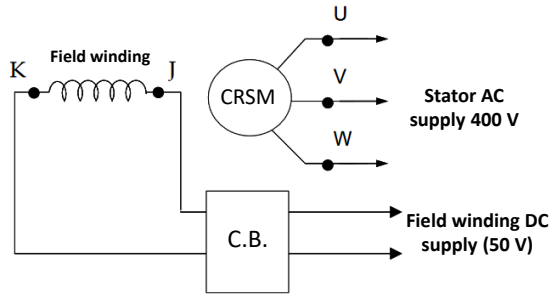

(c)

Fig. 4. a) Laboratory test bench, b) Tested CRSM and c) Electric scheme

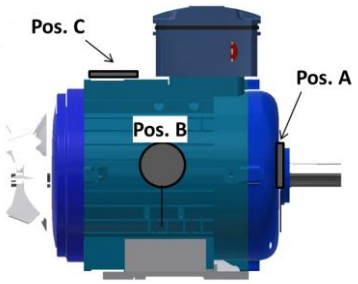

Fig. 5. Considered coil sensor positions

IV. Results and Discussion

This Section is divided into two parts: the first part includes the steady-state analyses that were performed considering the stray-flux signals captured at steady-state regime, both before and after synchronization (i.e. before and after feeding the field winding) [16]. Note that these analyses are based on the assumption that the motor operates as asynchronous during few seconds at steady-state, before moving to synchronous mode. This is not a realistic case since, in practice, the field winding is supplied before the steady-state is reached. The reason for including these analyses is twofold: on the one hand, to illustrate the differences between the spectra at asynchronous and synchronous modes, emphasizing the unsuitability of the analysis after synchronization for detecting damper faults due to the absence of significant current in the damper. The second objective is to show that a potential alternative to facilitate the damper fault detection would rely on leaving the motor under an asynchronous mode operation at steady-state (at least during a few seconds) since, as shown in the results, the resulting spectra of the asynchronous-mode signals would greatly facilitate the detection of a damper failure. This alternative may be especially useful in those motors in which the starting is too fast and starting current analysis may be difficult due to this fact.

The second part of the section is related to the time-frequency analyses of the stray-fluxes and currents under starting that were developed using the Short Time Fourier Transform (STFT), extending the analyses presented in [17]. In this section, a fault severity indicator is proposed to quantify the differences between the time-frequency analyses obtained for the tested CRSM.

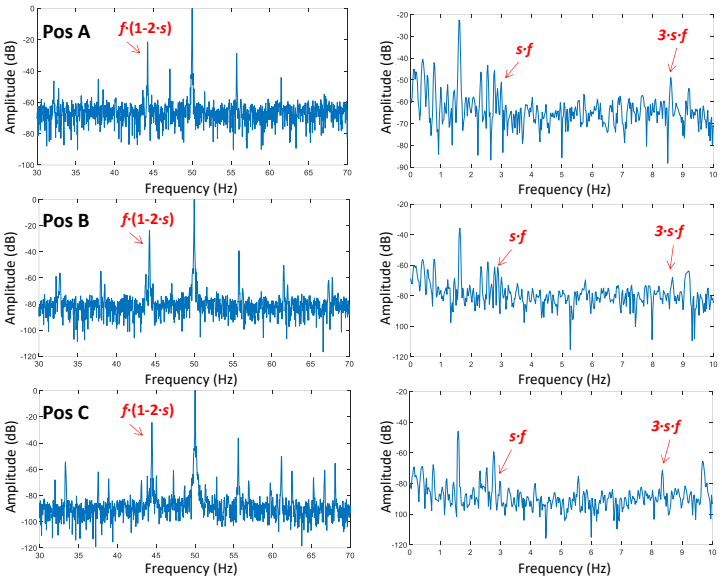

Fig.6. FFT analyses of the emf captured at steady-state for the CRSM1 (asynchronous operation, before synchronization)

A. *Steady-state analyses*

Fig. 6 shows the FFT of the emfs that were captured during the steady-state operation of CRSM1 before the motor was synchronized. During that short interval, the motor was operating in an asynchronous mode, so it is possible to observe the fault harmonics in the FFT spectra at all sensor positions. Note that, as expected, the radial components are more visible in those sensor positions in which the radial flux is mostly captured (mainly B and C), while the opposite happens for the axial (position A). In any case, at all sensor positions, a certain portion of axial and radial flux was captured.

Fig. 7 shows the same analyses as Fig.6 but for the machine operating after synchronization (i.e. synchronous mode). Note that, in this situation, the fault harmonics are not present in the FFT analyses since the damper cage has no current. Therefore, any damage in the damper is undetectable under this regime. One of the first conclusions of these facts is that, if it is possible to have the motor operating in an asynchronous mode at least during a short interval at steady-state, the FFT analysis of the steady-state flux data may bring very useful information for the diagnosis, especially in those cases in which the starting analysis (shown in the next section) may not be easily applicable due to a short starting duration.

B. *Transient analyses*

Figs. 8 to 10 show the time-frequency maps (region 0-250 Hz) resulting from the application of the STFT to the emf signals induced in the external coil sensor under the starting of the CRSM1. Each figure is referred to each of the sensor positions depicted in Fig. 5: at position A, the sensor mainly captures the axial flux, while at Position B and Position C, a mixture between axial and radial stray flux is measured.

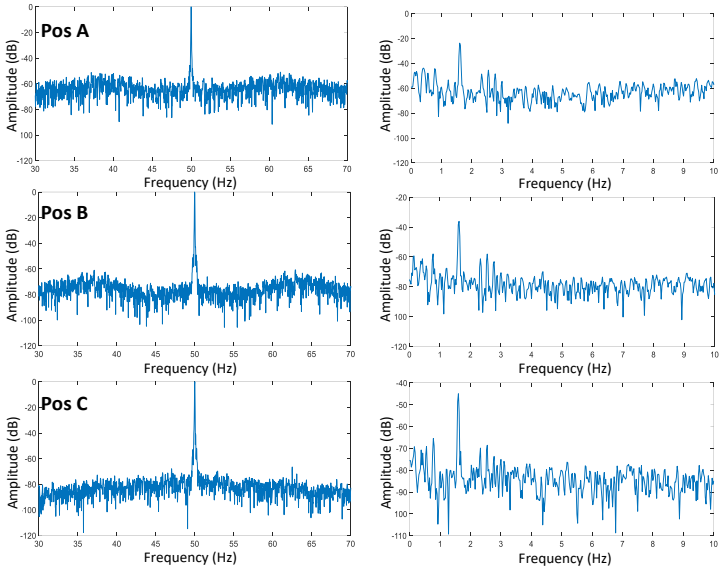

Figure 7. FFT analyses of the emf captured at steady-state for the CRSM1 (synchronous operation, after synchronization)

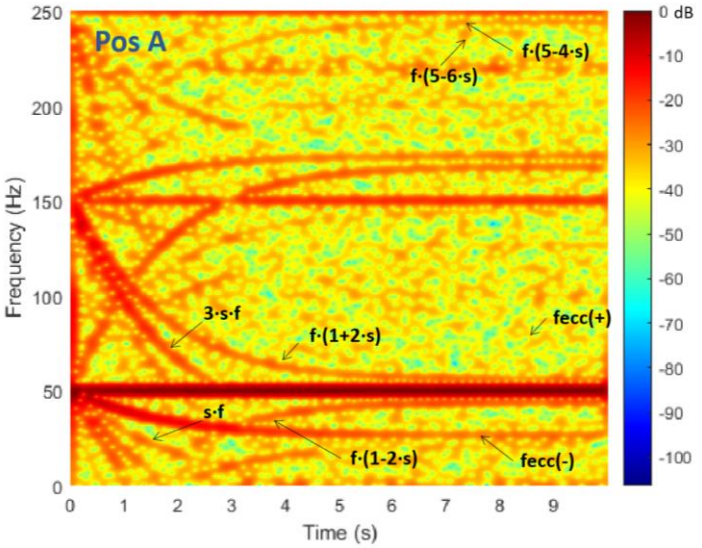

Fig. 8. STFT analysis of the emf signal under starting for the sensor located at position A (CRSM1).

With regards to the analyses shown in Figs. 8 to 10, note the rich harmonic content of the time-frequency maps resulting from the STFT of the emf signals induced by the stray-flux. These maps provide a lot of information related to the fault components present in the captured signals. This is extremely useful to determine the condition of the damper cage of the CRSM.

More specifically, note that, at position A (Fig. 8), the time-frequency analysis reflects the evolutions of most of the components, the theoretical evolutions of which are depicted in Fig. 1. These components are marked in the figure. It is especially interesting to emphasize the clear detection of the evolutions of the axial components $3 \cdot s \cdot f$ and, especially, $s \cdot f$, which are much better observed than in Figs 9 and 10 (corresponding to the other two sensor positions). This is because, as commented above, position A mainly captures the axial flux and, therefore, axial components are more noticeable in the analysis of the registered emf. Despite this fact, note that other components with radial nature (such as $f \cdot (1\text{-}2 \cdot s)$ and $f \cdot (1\text{+}2 \cdot s)$) are also observed at position A, but they are less clear than in the results corresponding to the other two sensor positions (see Fig. 9 and Fig. 10). The evolutions of other components linked with the damper cage failure, such as $f \cdot (5\text{-}6 \cdot s)$ and $f \cdot (5\text{-}4 \cdot s)$, among others, can be also detected and their detection serves to ratify the presence of the fault. Finally, it is worth mentioning that the evolutions of the components at $f_{ecc}(-)$ and $f_{ecc}(+)$ are also observed. As commented in other works referred to cage motors [15], these components were also amplified due to the presence of rotor bar faults.

With regards to position B (Fig. 9), the main difference versus the previous analysis relies on the fact that the radial components' evolutions (e.g. $f \cdot (1\text{-}2 \cdot s)$, $f \cdot (1\text{+}2 \cdot s)$, $f \cdot (5\text{-}4 \cdot s)$ and $f \cdot (5\text{-}6 \cdot s)$) are much more evident in the time-frequency maps, a fact that is explained by the higher portion of radial flux that is captured at this position. On the contrary, the evolutions of the axial components ($s \cdot f$ and $3 \cdot s \cdot f$) are hardly discernible.

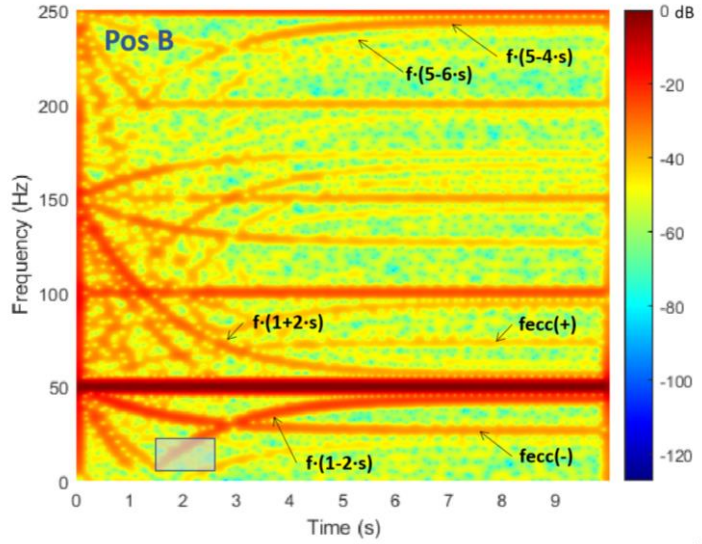

Fig. 9. STFT analysis of the emf signal under starting for the sensor located at position B (CRSM1).

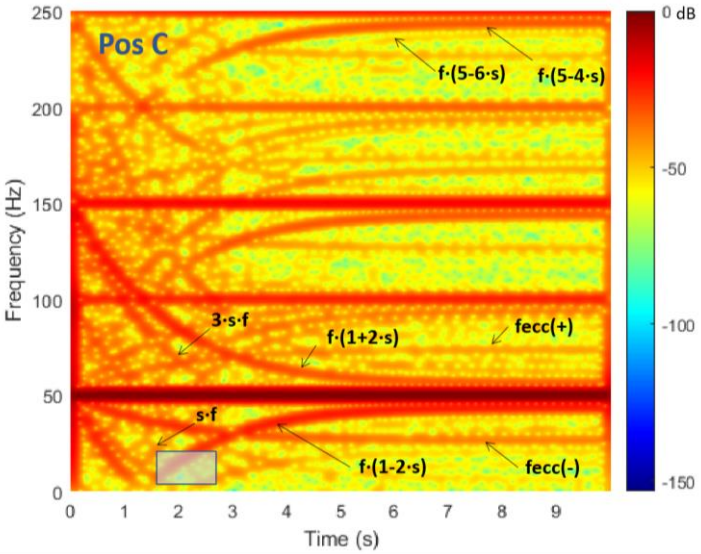

Fig. 10. STFT analysis of the emf signal under starting for the sensor located at position C (CRSM1).

Finally, the results for position C are rather similar to those of position B. The main difference is that, at position C, it is possible to better observe the axial components' evolutions (especially $3{\cdot}s{\cdot}f$), probably because a higher portion of axial flux is captured at that sensor location.

All in all, the stray flux analyses show that plenty of information is obtained, regarding the condition of the damper cage. Even if different components are better detected, depending on the sensor position, the combined analysis of the information obtained at all sensor positions increases the reliability of the diagnostic, since it is supported by the detection of components of different nature.

Fig. 11 shows the STFT analysis of the starting current for the CRSM1. First, note the less rich harmonic content of the time-frequency map, in comparison with those of Figs. 8 to 10. In other words, fewer evolutions are observed under starting, compared to the previous figures. Second, note that there are some components which are not noticeable in the time-frequency analysis of the starting current. In this regard, the evolutions of the axial components at $s{\cdot}f$ and $3{\cdot}s{\cdot}f$ are not observed, while the eccentricity/misalignment components at $f_{ecc}(-)$ and $f_{ecc}(+)$ are less distinguishable. On the contrary, the evolutions of the main sideband harmonics at $f{\cdot}(1{\pm}2{\cdot}s)$ are observed much more clearly than for the stray flux analyses. Indeed, the evolutions of other sideband families such as $f{\cdot}(1{\pm}4{\cdot}s)$, $f{\cdot}(1{\pm}6{\cdot}s)$ and even $f{\cdot}(1{\pm}8{\cdot}s)$ are also clearly noticeable.

Figs. 12 to 14 show the STFT analyses of the emf signals under starting for the CRSM2 (started at rated voltage). Note that CRSM2 had a characteristic that made them different from CRSM1: it had certain remanent magnetism in the rotor caused by previous experimentation over years. Due to this fact, the starting of this machine was much faster and, furthermore, the machine was auto-synchronized when the steady-state was reached, without needing to feed the field winding. The main effect of this remanent magnetism, with regards to the detection of damper failures based on starting analysis, is that the transient is much faster (<1 sec), so it is almost impossible to identify the rotor fault components' evolutions, as observed in Figs. 12 to 14. Only the eccentricity components at steady-state are visible.

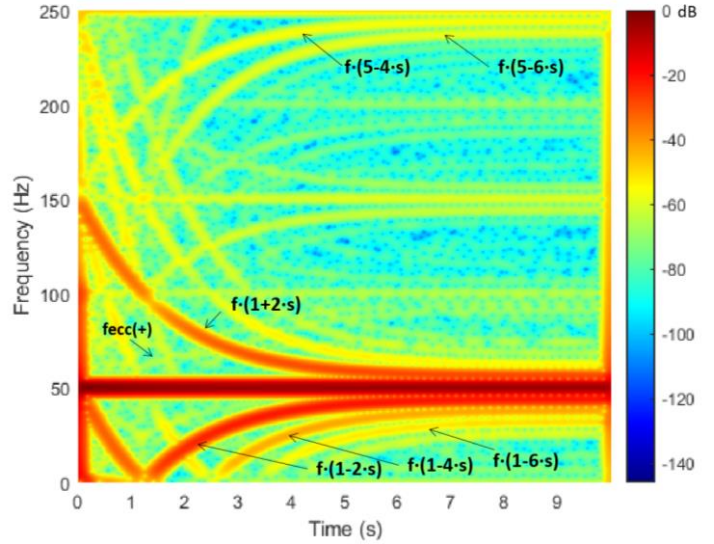

Fig. 11. STFT analysis of the starting current for the CRSM1.

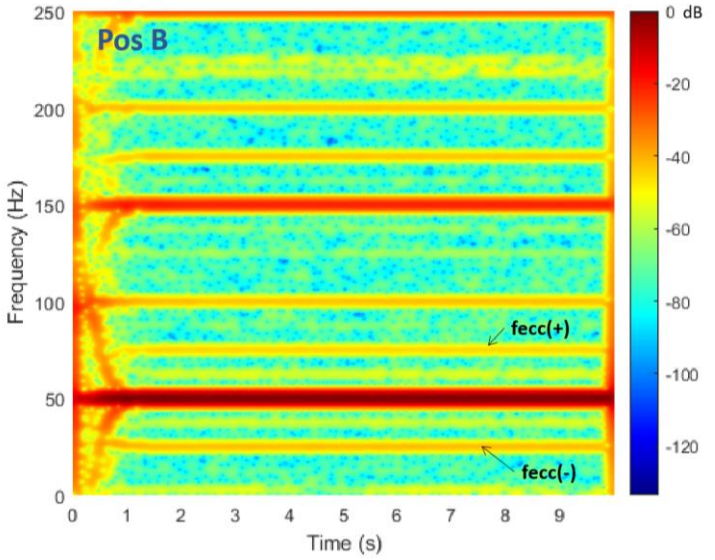

Fig. 13. STFT analysis of the emf signal under starting for the sensor located at position B (CRSM2, remanent magnetism).

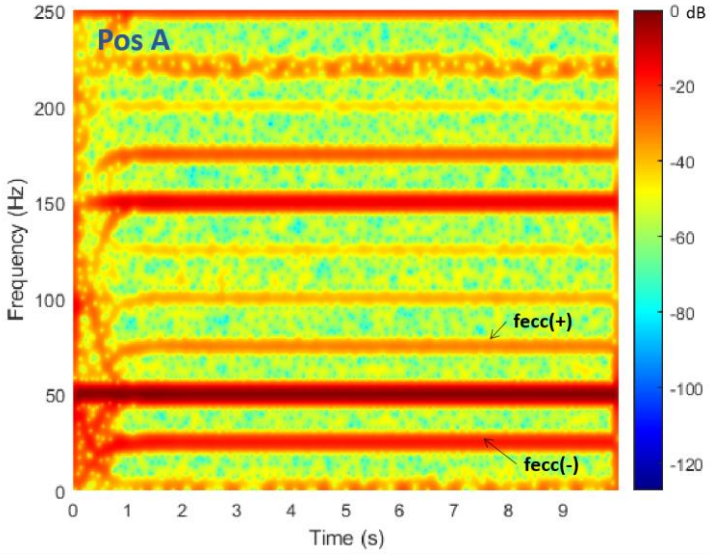

Fig. 12. STFT analysis of the emf signal under starting for the sensor located at position A (CRSM2, remanent magnetism).

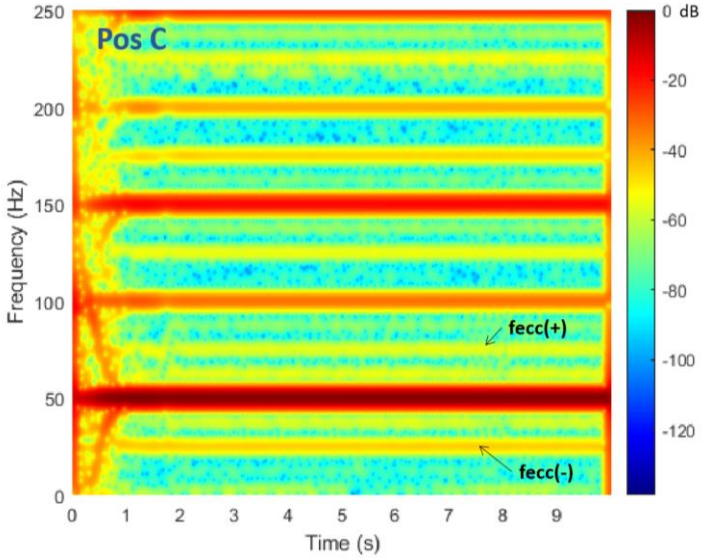

Fig. 14. STFT analysis of the emf signal under starting for the sensor located at position C (CRSM2, remanent magnetism).

The time-frequency analysis of the starting current for CRSM2 yields similar problems to identify the fault harmonics, since the transient was too short, due to the effect of the remanent magnetism, as shown in Fig. 15.

A possible solution to the problem caused by the remanent magnetism, which makes the application of the proposed diagnosis methodology difficult, relies on making the startup duration longer. This can be done by supplying the machine with a reduced voltage under starting. This leads to a longer duration of the starting current signal and enables to better identify the evolutions of the fault components. In that way, it is possible to determine the condition of the damper based on the proposed methodology. This is illustrated in Figs. 16 to 18, which depict the STFT analyses of the emf during the starting for the CRSM2, when this machine was started using a reduced voltage (~60% of the rated voltage is considered in the figures, although other reduced voltage levels are possible, provided that the starting duration is at least 1-1,5 s). Note the longer duration of the transient, which allows a clear identification of the evolutions of the fault components linked to damper damages (the theoretical evolutions of which were shown in Fig.1).

A simple comparison between Figs. 16 to 18 and Figs. 8 to 10 reveals a healthier condition of the damper of CRSM2 compared to that of CRSM1: the fault related patterns for CRSM1 have greater intensities than those of CRSM2, as observed in those graphs (compare, for instance, the $f\cdot(1\text{-}2\cdot s)$ between Fig.9-Fig.17 and Fig. 10-Fig. 18. This is coherent with the considerations carried out above about the previous conditions of each damper. Note that, despite the healthier state of the damper of CRSM2, traces of the fault components are observable, probably due to the inherent asymmetry due to the slotting of the field winding in these machines (Fig. 2). In any case, to quantify the differences in the conditions of the damper windings of both machines, a fault severity indicator is proposed. This indicator is defined as the maximum energy density (related to that of the fundamental component) of a specific area of the time-

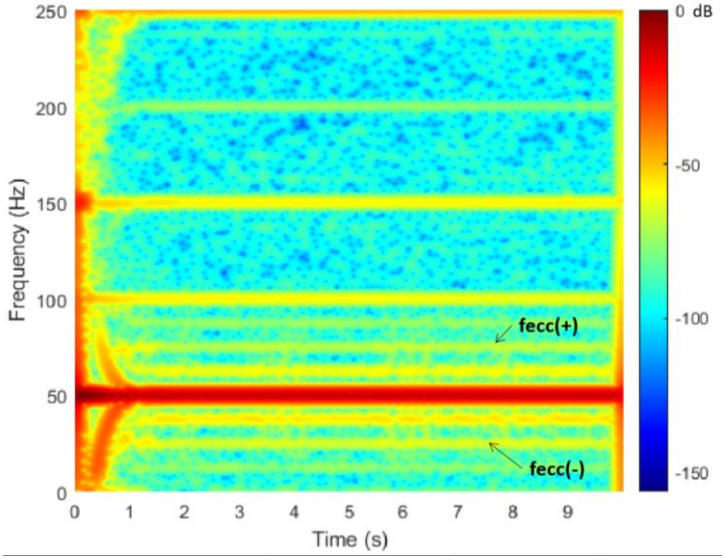

Fig. 15. STFT analysis of the starting current for the CRSM2 affected by remanent magnetism (rated voltage).

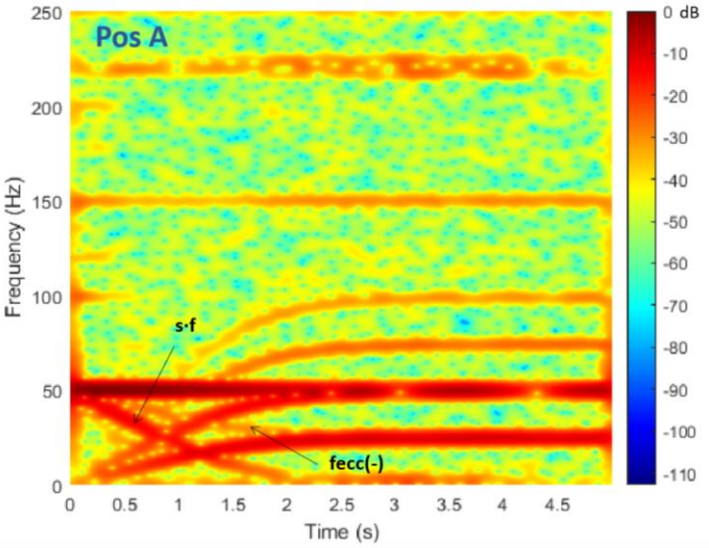

Fig. 16. STFT analysis of the emf signal under a reduced voltage starting for the sensor located at position A (CRSM2, residual magnetism).

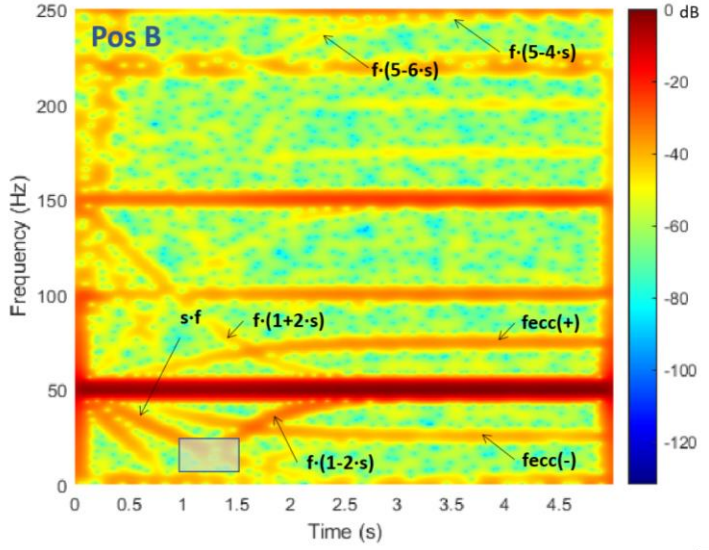

Fig. 17. STFT analysis of the emf signal under a reduced voltage starting for the sensor located at position B (CRSM2, residual magnetism).

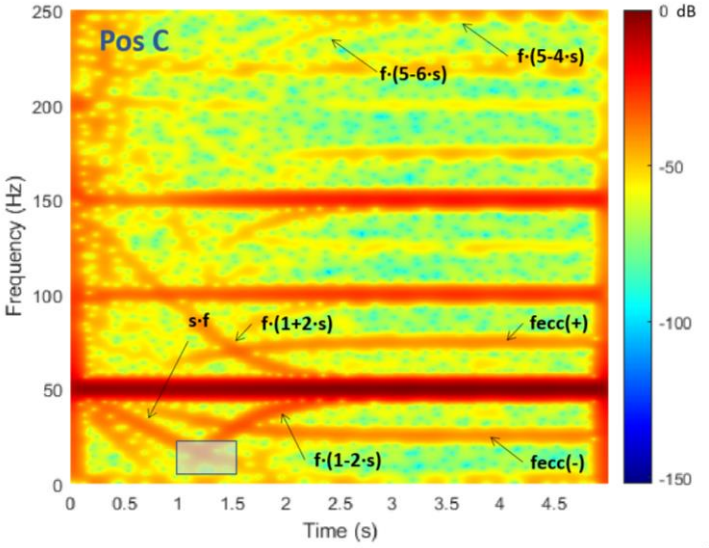

Fig. 18. STFT analysis of the emf signal under a reduced voltage starting for the sensor located at position C (CRSM2, residual magnetism).

frequency map. The considered area to compute the indicator is that shadowed in Figs.9-10 and 17-18. It has been selected since it is trespassed by the most relevant fault harmonic (f·(1-2·s)) under starting (this is why only positions B and C have been considered, since at position A this radial component is less observable). The exact definition of the indicator is given by (1) (where $En_{i,j}$ is the energy density at the (i, j) coordinate of the time-frequency map, t_0 and t_f are, respectively, the initial and final x-samples defining the considered t-f area and f_0 and f_f are, respectively, the initial and final y-samples defining to the considered t-f area). As a reference, the considered time interval for the selected time-frequency area is between 30% and 50% of the starting duration and the frequency range between 5 and 25 Hz.

$$\gamma_A = Max(En_{i,j})_{i=t_0 \cdots t_f;\ j=f_0 \cdots f_f} \quad (1)$$

Table I shows the value of the considered fault indicator for each machine. To compute its value, different supply voltages have been considered in order to study the its possible influence on the indicator value. The results prove the consistency of the fault indicator: for each machine, its value remains quite stable, regardless of the considered position (B, C) and supply voltage level. Moreover, its value reveals clear differences between CRSM1 and CRSM2, showing lower values for this latter machine, which indicates a healthier condition of its damper in agreement with that stated above.

TABLE I.
COMPUTATION OF FAULT SEVERITY INDICATOR FOR CRSM1 AND CRSM2 AT EACH SENSOR POSITION AND FOR DIFFERENT SUPPLY VOLTAGES

CRSM2	
Pos B	
Supply voltage (% of rated voltage)	**INDICATOR**
100%	**-36.26**
80%	**-38.13**
60%	**-36.4**
Pos C	
Supply voltage (% of rated voltage)	**INDICATOR**
100%	**-36.41**
80%	**-38.57**
60%	**-35.36**
CRSM1	
Pos B	
Supply voltage (% of rated voltage)	**INDICATOR**
100%	**-27.22** **(+24.9%)**
80%	**-27.45** **(+28%)**
60%	**-28.3** **(+22.2%)**
Pos C	
Supply voltage (% of rated voltage)	**INDICATOR**
100%	**-26.33** **(+27.6%)**
80%	**-26.05** **(+32.4%)**
60%	**-27.8** **(+29.8%)**

Finally, Fig. 19 is referred to the STFT analysis of the starting current for a machine started under reduced voltage conditions. Note that, in that figure, most of the fault components associated with the damper fault can be identified, as it happened in Fig. 11. In conclusion, a possible solution in machines with remanent magnetism is to perform this type of startup modality, so that the asynchronous starting is longer and, hence, the fault components are better identifiable.

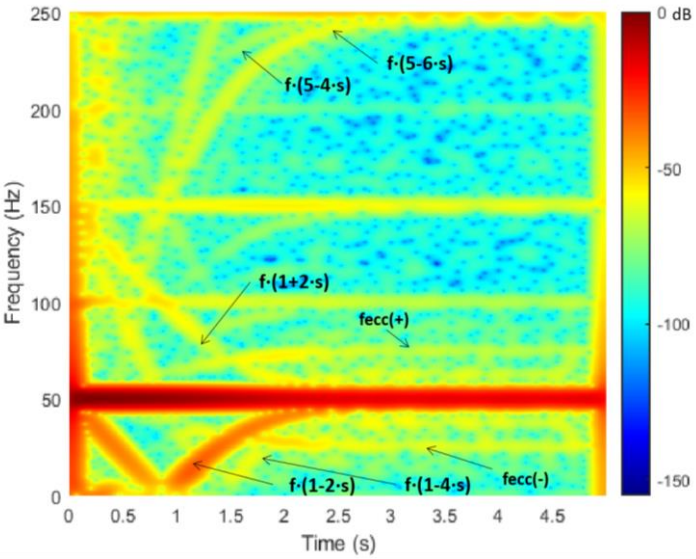

Fig. 19. STFT analysis of the starting current for the CRSM2 affected by remanent magnetism (reduced voltage).

V. CONCLUSIONS

This paper has presented a comparison between stray flux and current analyses under starting for the detection of damper failures in CRSM.

The analysis of the starting transient has been proven as a reliable way for diagnosing damper damages in synchronous motors. This work has shown the qualitative differences obtained from the stray flux analyses for two CRSM with different levels of damper failures and has proposed a fault severity indicator to quantify the level of damper damage.

.In comparison with starting current analyses, the time-frequency analysis of the stray flux signals are much richer in harmonic content, a fact that contributes to enhance the reliability in the diagnostic of the failure.

In addition, the fact that the sensor position determines the fault components that will be better observed in the time-frequency analyses has a positive implication: if the information is obtained from different sensor positions, more fault related components of different nature (axial/radial) will be observed and, therefore, the diagnosis will be more robust, since it will not only rely on the detection of a single or of few components.

On the other hand, starting current analysis, although less rich in harmonic content, yields very clear evolutions of the main fault related components (especially, of the main sidebands).

Additionally, the effect on the remanent magnetism in the rotor is also considered in the work. This phenomenon may complicate the diagnosis since it can make the startup much shorter, enabling a fact synchronization of the machine (even before feeding the field winding). To solve this problem, potential solutions, such as starting the machine under a

reduced voltage, are proven to be useful. This enables a longer duration of the starting and, consequently, a better visualization of the fault components evolutions. Results reveal no significant influence of the supply voltage level on the results of the methodology (both qualitative and quantitative).

In consequence, the combined analysis of currents and stray flux signals under starting, if feasible, reveals itself as a promising tool for the reliable diagnostic of the damper fault, the implications of which may be very severe for the integrity of the machine and of the process itself.

VI. REFERENCES

[1] H.A. Toliyat, S. Nandi, S. Choi, and H. Meshgin-Kelk, *Electric Machines: Modelling, Condition Monitoring and Fault Diagnosis*. New York: Taylor & Francis Group. 2013.

[2] E.W. Kimbark, "Damper Windings and Damping," in *Power System Stability*, IEEE, 1995, pp.214-246.

[3] B. Amin, *Induction Motors: Analysis and Torque Contro*l, New York: Springer. 2002.

[4] J. Antonino-Daviu, V. Fuster-Roig, S. Park, Y. Park, H. Choi, J. Park, and S.B. Lee, "Electrical Monitoring of Damper Bar Condition in Salient Pole Synchronous Motors without Motor Disassembly," *in IEEE Transactions on Industry Applications*, vol. 56, no. 2, pp. 1423-1431, March-April 2020.

[5] J. Yun, S.W. Park, C. Yang, S.B. Lee, J.A. Antonino-Daviu, M. Sasic, and G.C. Stone "Airgap Search Coil-Based Detection of Damper Bar Failures in Salient Pole Synchronous Motors," *IEEE Trans. Ind. Appl.*, vol. 55, no. 4, pp. 3640-3648, July/Aug. 2019.

[6] J. A. Antonino-Daviu, M. Riera-Guasp, J. Pons-Llinares, J. Roger-Folch, R. B. Pérez and C. Charlton-Pérez, "Toward Condition Monitoring of Damper Windings in Synchronous Motors via EMD Analysis," in *IEEE Transactions on Energy Conversion*, vol. 27, no. 2, pp. 432-439, June 2012.

[7] Y. Park, S. B. Lee, J. Yun, M. Sasic and G. C. Stone, "Air Gap Flux-Based Detection and Classification of Damper Bar and Field Winding Faults in Salient Pole Synchronous Motors," in IEEE Transactions on Industry Applications, vol. 56, no. 4, pp. 3506-3515, July-Aug. 2020.

[8] M. Faizan Shaikh, J. Park and S. B. Lee, "A Non-Intrusive Leakage Flux based Method for Detecting Rotor Faults in the Starting Transient of Salient Pole Synchronous Motors," in *IEEE Transactions on Energy Conversion*, Accepted for publication. 2020.

[9] J.A. Ramirez-Nunez, J.A. Antonino-Daviu, V. Climente-Alarcón, A. Quijano-López, H. Razik, R.A. Osornio-Rios, R. de J. Romero-Troncoso "Evaluation of the Detectability of Electromechanical Faults in Induction Motors Via Transient Analysis of the Stray Flux," in *IEEE Transactions on Industry Applications*, vol. 54, no. 5, pp. 4324-4332, Sept.-Oct. 2018.

[10] I. Zamudio-Ramirez, J. A. Antonino-Daviu, R. A. Osornio-Rios, R. de Jesus Romero-Troncoso and H. Razik, "Detection of Winding Asymmetries in Wound-Rotor Induction Motors via Transient Analysis of the External Magnetic Field," in *IEEE Transactions on Industrial Electronics*, vol. 67, no. 6, pp. 5050-5059, June 2020.

[11] J. Antonino-Daviu, V. Climente-Alarcón, J. Pons-Llinares, M. Pineda-Sanchez, "Transient-based analysis for the detection of broken damper bars in synchronous motors," *Mechanical Systems and Signal Processing*, Volume 34, Issues 1–2, January 2013, Pages 367-377.

[12] R. Romary, R. Pusca, J. P. Lecointe, and J. F. Brudny, "Electrical machines fault diagnosis by stray flux analysis," in *Proc. IEEE WEMDCD*, Paris, France, Mar. 11–12, 2013, pp. 247–256.

[13] A. Ceban, R. Pusca and R. Romary, "Study of Rotor Faults in Induction Motors Using External Magnetic Field Analysis*", IEEE Trans. Ind. Electronics*, vol. 59, no. 5, pp. 2082-2093, 2012.

[14] Y. Park, H. Choi, J. Shin, J. Park, S. B. Lee and H. Jo, "Airgap Flux Based Detection and Classification of Induction Motor Rotor and Load Defects During the Starting Transient," *in IEEE Transactions on Industrial Electronics*, vol. 67, no. 12, pp. 10075-10084, Dec. 2020.

[15] K. N. Gyftakis, P. A. Panagiotou and S. B. Lee, "The Role of the Mechanical Speed Frequency on the Induction Motor Fault Detection via the Stray Flux," *2019 IEEE 12th International Symposium on Diagnostics for Electrical Machines, Power Electronics and Drives (SDEMPED)*, Toulouse, France, 2019, pp. 201-207.

[16] H. Castro-Coronado, J. Antonino-Daviu, A. Quijano-López, V. Fuster-Roig and P. Llovera-Segovia, "Evaluation of the Detectability of Damper Cage Damages in Synchronous Motors through the Advanced Analysis of the Stray Flux," 2020 IEEE Energy Conversion Congress and Exposition (ECCE), Detroit, MI, USA, 2020, pp. 2058-2063.

[17] H. Castro-Coronado, J. Antonino-Daviu, A. Quijano-Lopez, P. Llovera-Segovia and V. Fuster-Roig, "Stray-flux and Current Analyses under Starting for the Detection of Damper Failures in Cylindrical Rotor Synchronous Machines," 2020 International Conference on Electrical Machines (ICEM), Gothenburg, 2020, pp. 1475-1480.

VII. BIOGRAPHIES

Habib Castro Coronado received the Bs. Degree in Electromechanical Engineering from the Instituto Tecnológico y de Estudios Superiores Monterrey (ITESM), Campus Monterrey, Mexico, in 2009 and his M. Sc. degree in Maintenance Engineering from Universitat Politécnica de Valencia (UPV), Spain. His Master thesis was focused on the applicability of the stray flux analysis for fault diagnosis in synchronous machines. Between 2012 and 2017, he worked as maintenance supervisor and product engineer for Komatsu Mexico. He has recently joined the RAM and LCC department of Stadler Rail Valencia where he collaborates in the development of maintenance plans for railway vehicles.

Jose A. Antonino-Daviu received the M.Sc. and Ph.D. degrees in electrical engineering, both from the Universitat Politècnica de València, Valencia, Spain, in 2000 and 2006, respectively. He has worked for IBM, involved in several international projects. He is currently a Full Professor in the Department of Electrical Engineering, Universitat Politècnica de València. He was an Invited Professor at Helsinki University of Technology, Finland, in 2005 and 2007, Michigan State University, USA, in 2010, Korea University, South Korea, in 2014, Université Claude Bernard Lyon 1, France, and Coventry University, U.K., in 2016. He is a coauthor of more than 200 papers published in technical journals and conference proceedings. He is also the coauthor of one international patent.

Dr. Antonino-Daviu is an Associate Editor of the IEEE TRANSACTIONS ON INDUSTRIAL INFORMATICS and a member of the Editorial Board. He received the IEEE Second Prize Paper Award of the Electric Machines Committee of the IEEE Industry Applications Society (2013). He also received the Best Paper Award in the conferences IEEE ICEM 2012, IEEE SDEMPED 2011and IEEE SDEMPED 2019 and the "Highly Commended Recognition" of the IET Innovation Awards in 2014 and in 2016. He was the General Co-Chair of SDEMPED 2013 and is a member of the Steering Committee of IEEE SDEMPED. In 2016, he received the Medal of the Spanish Royal Academy of Engineering (Madrid, Spain) for his contributions in new techniques for predictive maintenance of electric motors. In 2018, he has been awarded with the prestigious 'Nagamori Award' from the Nagamori Foundation (Kyoto, Japan). In 2019, he received the SDEMPED diagnostic achievement Award (Toulouse, France) for his contributions to electric motors advanced diagnosis.

Alfredo Quijano-Lopez was born in 1960 in Valencia, Spain. He received the Electrical Engineer degree and the Ph.D. degree from Universitat Politècnica de València, in 1986 and 1992, respectively. He is the Head of the Instituto Tecnológico de la Energía. He is also a professor and a researcher at the Universitat Politècnica de València in the Electrical Engineering Department. His current research activity is focused on applied research for the Energy area and the electrical technology including renewable energies, high voltage, metrology, new materials and applications and research results transfer to companies.

Pedro Llovera-Segovia received the M.Sc. in electrical engineering from the Universitat Politècnica de València, Valencia, Spain, in 1997 and the Ph.D. in electrical engineering from Universitat Politecnica de Valencia, Spain and Université Paris XI, France in 2002. He is currently a permanent researcher and teacher at the Department of Electrical Engineering of the Universitat Politècnica de València. He has published more than 20 papers in international indexed journals and has 4 patents.

He has taken part in multiple projects, most of the in collaboration with industry. He is expert in insulating materials for H.V. applications and industrial electrostatics, among other areas.

Vicente Fuster-Roig was born in 1965 in Valencia, Spain. He is a permanent researcher and teacher of the Universitat Politècnica de València where he obtained the Engineer degree in 1991 and the Ph.D. degree in 1996 on the topic of power quality. He has participated as the main researcher on many applied projects with industry, mainly on electromagnetic compatibility, electric measurements, electromagnetic modelling, insulation ageing, high currents and high voltage. He is currently part of the scientific direction of the Instituto Tecnológico de la Energía and he is carrying research on electromagnetic compatibility, insulation materials and smart grids.

Luis Serrano-Iribarnegaray was born in 1949 in Bilbao, Spain. He received the electrical and doctoral engineering degrees from the universities of Bilbao (in 1971) and Madrid (in 1978), Spain, respectively. since 1982, he has held the chair for theory and control of electrical machines at the Universidad Politecnica de Valencia , Spain and has been the scientist responsible in Spain for various international projects on electronic control of electrical machines, supported by the Euro-pean Union.

Larisa Dunai (M´19), Associate Professor at UPV, obtained her MSc degree in Electronic Engineering in 2003 from Technical University of Moldova and a Master degree in Electronic Engineering in 2004 at the same university. After obtaining the MSc degree joined the Technical University of Moldova as Assistant professor at the Radio electronics and Telecommunications Department. In 2007 she started working as a researcher in the Research Center in Graphic Technology (CITG) of the Universidad Politecnica de Valencia. In November 2008 she joined the UPV as an Assistant professor of Graphic Design Department. In 2010 obtained her PhD at Universitat Politècnica de València. In 2013 she received the MIT Innovators Award for Spain and in 2014 the Michael Richey Medal from Royal Institute of Navigation.